Electronic Supplementary Material (ESI) for Dalton Transactions.
This journal is © The Royal Society of Chemistry 2018

Supporting Information for

Dramatically enhanced visible-light driven H_2 evolution by anchoring TiO_2 nanoparticles on the molecularly grafted carbon nitride nanosheets via a multiple modification strategy

Jingyu Wang,*[a] Zili Xu,[a] Chuansheng Zhuang,[b] Heng Wang,[a] Xiaochan Xu,[a] Bien Tan,[a] Tao Li,*[a] and Tianyou Peng*[b]

[a] Key Laboratory of Material Chemistry for Energy Conversion and Storage (Ministry of Education), School of Chemistry and Chemical Engineering, Huazhong University of Science and Technology, Wuhan 430074, Hubei, China. E-mail: wangjingyu@hust.edu.cn; taoli@mail.hust.edu.cn.

[b] College of Chemistry and Molecular Sciences, Wuhan University, Wuhan 430072, P. R. China. E-mail: typeng@whu.edu.cn.

Figures

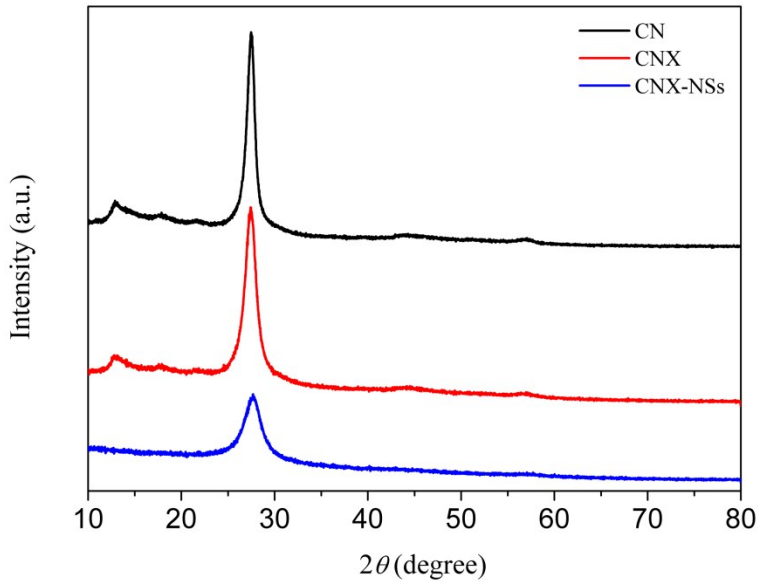

Figure S1. XRD patterns of bulk CN, bulk CNX, and CNX-NSs.

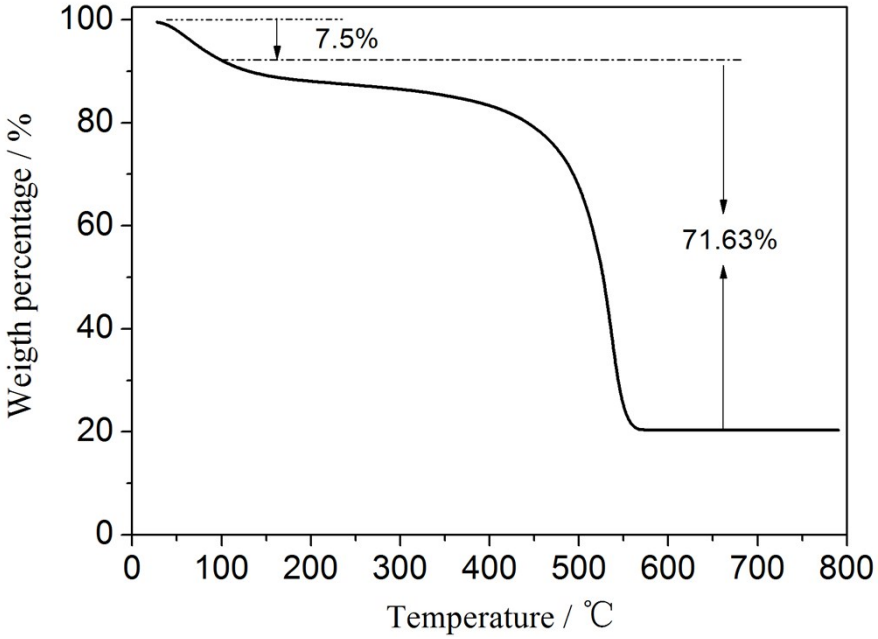

Figure S2. TGA curve of the TiO_2/CNX-NSs hybrid with the theoretical mass ratio of TiO_2 to CNX-NSs at 1:3.

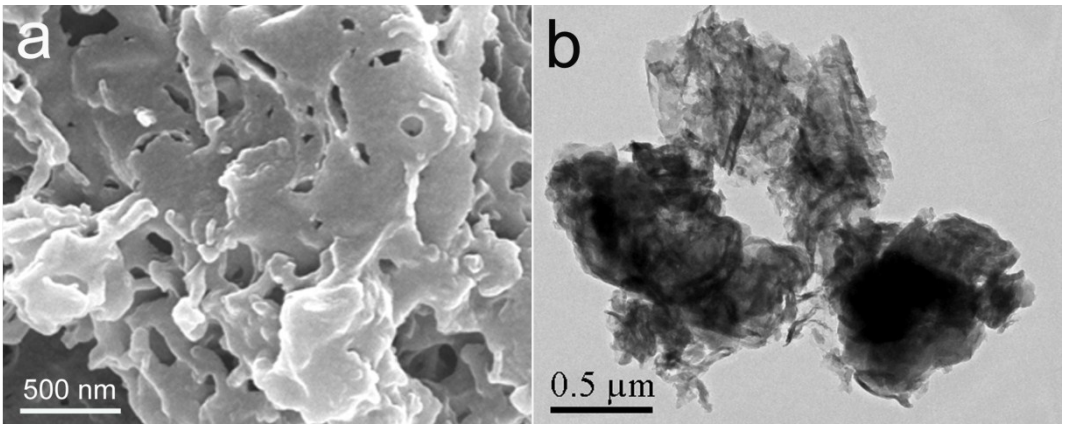

Figure S3. SEM (a) and TEM (b) images of bulk CNX.

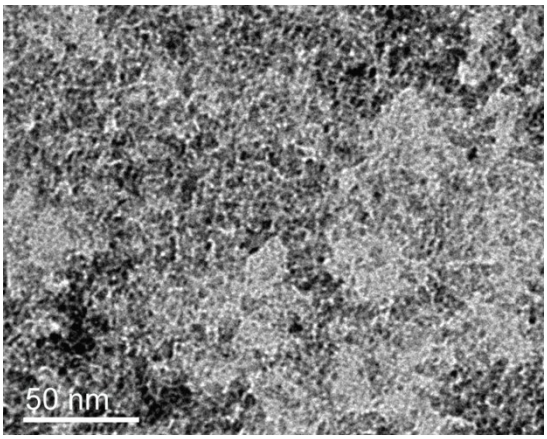

Figure S4. TEM image of TiO_2 hydrosol.

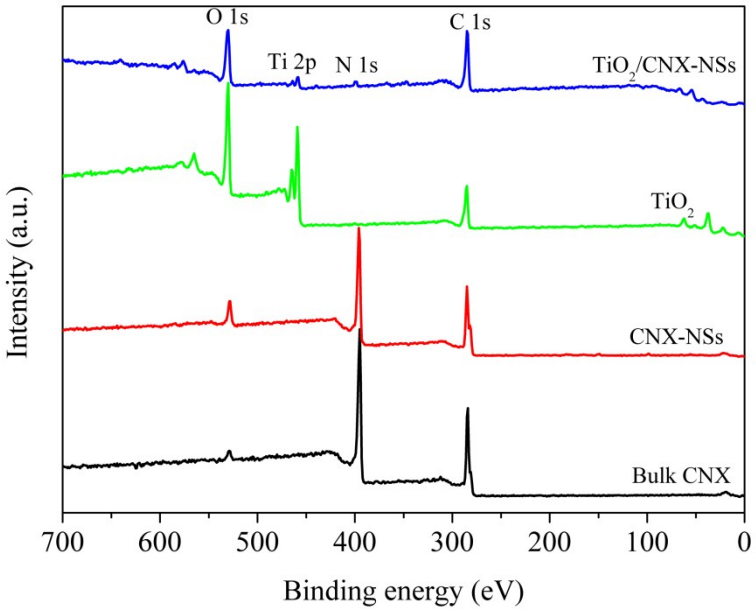

Figure S5. The XPS survey spectra of bulk CNX, CNX-NSs, TiO_2, and TiO_2/CNX-NSs (3:1) hybrid.

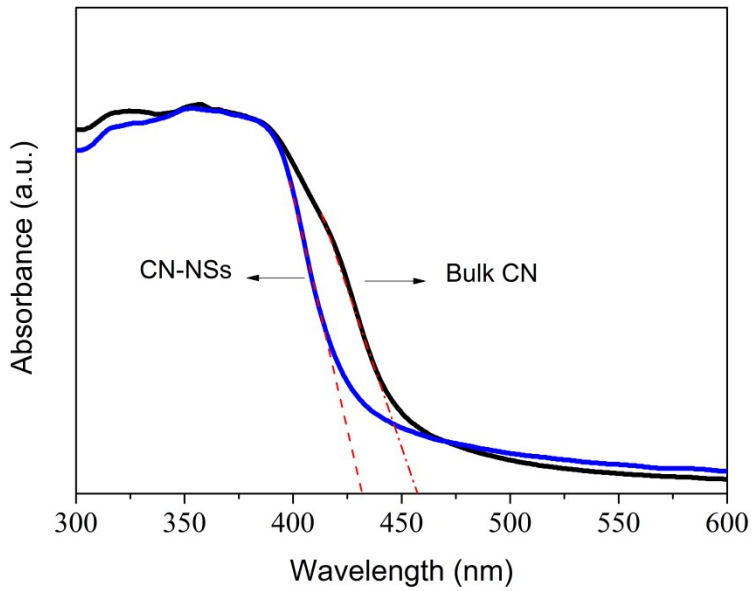

Figure S6. Comparison of UV-vis DRS of CN materials before and after liquid-phase exfoliation.

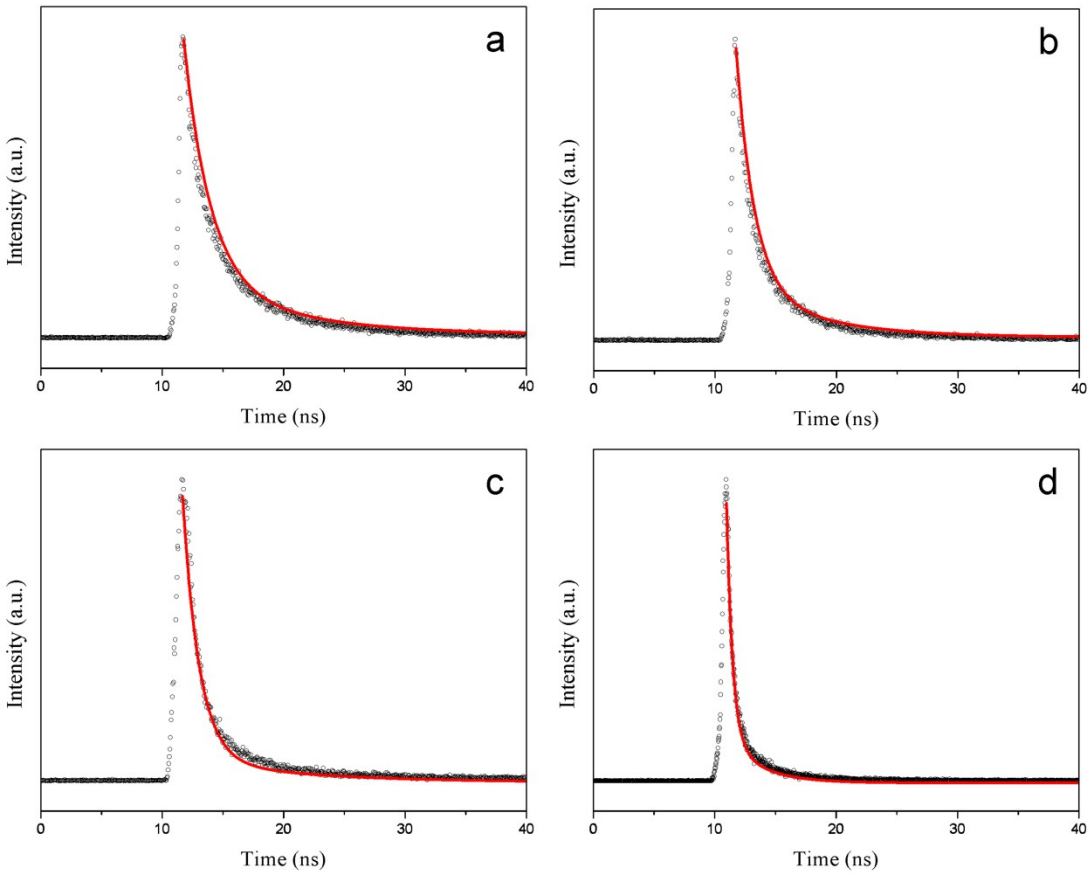

Figure S7. The transient-state photoluminescence decay spectra of bulk CN (a), bulk CNX (b), TiO_2 (c), and TiO_2/CNX-NSs hybrid (d).

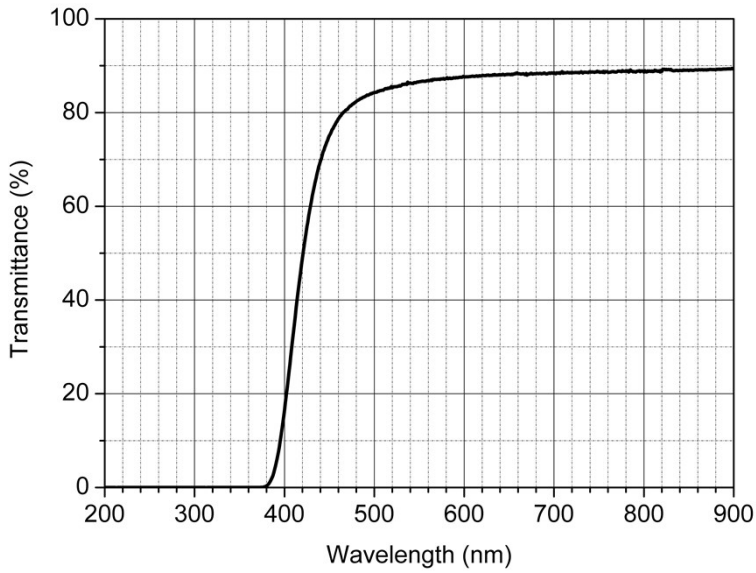

Figure S8. UV-Vis transmittance spectrum of the 400 nm cutoff filter that installed outside the 300 W Xe lamp.

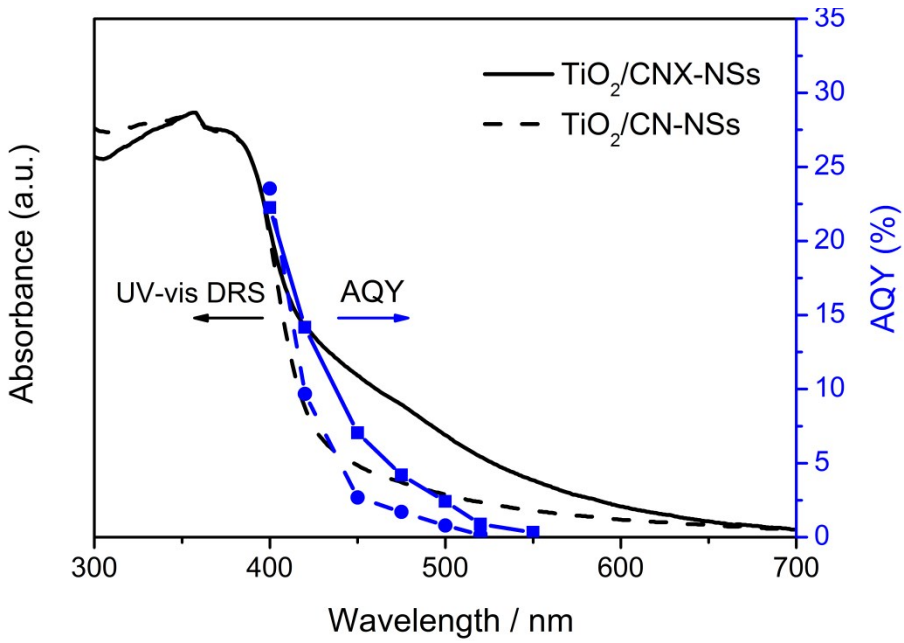

Figure S9. Wavelength-dependent AQY of H_2 production by the TiO_2/CN-NSs hybrid using the correspondingband-pass filters of λ ± 15 nm. The UV–vis DRS is overlapped for comparison.

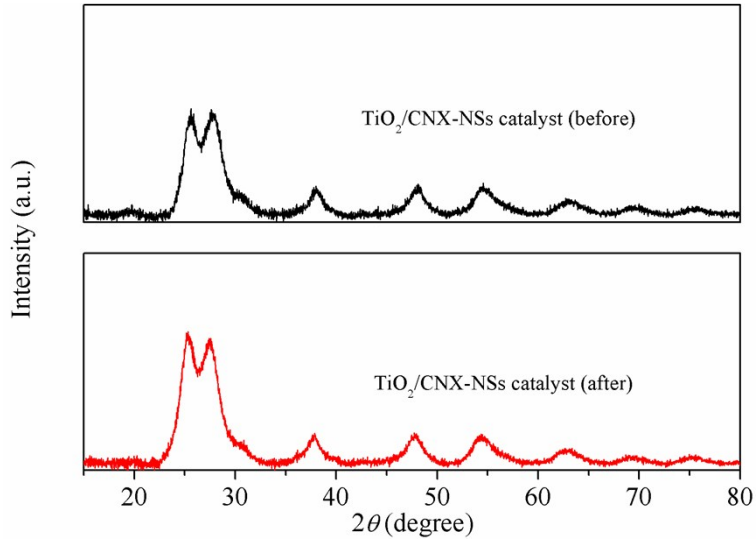

Figure S10. XRD patterns of the TiO_2/CNX-NSs hybrid before and after cycles of photocatalytic reaction.

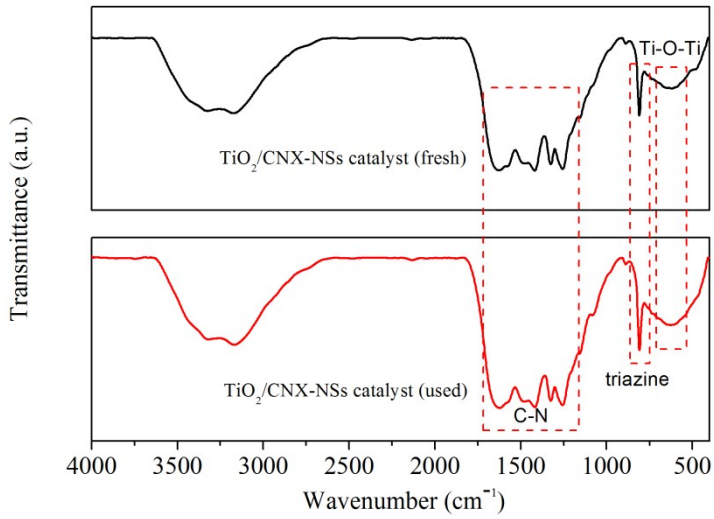

Figure S11. FT-IR spectra of the TiO_2/CNX-NSs hybrid before and after cycles of photocatalytic reaction.

Table S1. Decay lifetimes related to the transient-state photoluminescence spectra of bulk CN, bulk CNX, TiO_2, and TiO_2/CNX-NSs hybrid.

Samples	$\tau_{1(ns)}$	A_1(%)	$\tau_{2(ns)}$	A_2(%)	$<\tau>$ (ns)
bulk CN	2.16	52.51	8.45	47.49	7.06
bulk CNX	1.51	51.95	6.55	48.05	5.55
TiO_2	1.36	61.37	9.58	38.63	8.07
TiO_2/CNX-NSs	0.50	49.29	2.73	50.71	2.39

The average lifetime could be calculated by the following equation:

$$<\tau>=\frac{A_1\tau_1^2+A_2\tau_2^2}{A_1\tau_1+A_2\tau_2}$$

Where $<\tau>$, τ and A represent the intensity-average lifetime, decay time and relative magnitude of components, respectively.

Table S2. Comparisons of H_2 production rate with the analogue photocatalysts in the recent literatures.

Photocatalyst	(mg)	Co-catalyst	Light source	Scavenger	H_2 (μmol/h)	AQY	Ref
C-TiO_2/g-C_3N_4	50	Pt	300W Xe lamp (≥420 nm)	TEOA	57.28	6.2% at 420 nm	[1]
N-TiO_2/g-C_3N_4	3	-	Xenon lamp (≥420 nm)	methanol	0.89	1.2% at 420nm	[2]
g-C_3N_4/TiO_2	100	Pt	300W Xe lamp (≥420 nm)	TEOA	68.76	-	[3]
TiO_2@g-C_3N_4 nanospheres	10	-	300W Xe lamp (≥420 nm)	methanol	0.356	-	[4]
3D g-C_3N_4/TNA	100	Pt	300W Xe lamp (≥400 nm)	methanol	24.3	-	[5]
g-C_3N_4/TiO_2	45	Pt	800W Xe-Hg lamp(≥420nm)	TEOA	1.35	-	[6]
g-C_3N_4/TiO_2	100	Pt	500W Xe lamp (＞420 nm)	methanol	35.44	-	[7]
g-C_3N_4/TiO_2 Nanofibers	5	Ag	300W Xe lamp (≥400 nm)	TEOA	0.305	-	[8]
g-C_3N_4/Ni_3C	50	Ni_3C	350W Xe lamp (＞420 nm)	TEOA	15.18	0.40% at 420 nm	[9]
$Ni_{12}P_5$/g-C_3N_4	50	$Ni_{12}P_5$	350W Xe lamp (＞420 nm)	TEOA	6.33	-	[10]
NiS/g-C_3N_4	50	NiS	350W Xe lamp (＞420 nm)	TEOA	29.68		[11]
g-C_3N_4/carbon /NiS	50	NiS	300W Xe lamp (≥420 nm)	TEOA	18.32	-	[12]
g-C_3N_4-Ni-NiS	50	Ni/NiS	300W Xe lamp (＞420 nm)	TEOA	25.75		[13]
NiS/g-C_3N_4 /$SrTiO_3$	50	Pt	300W Xe lamp (≥420 nm)	methanol	86.135	-	[14]
Na-doped g-C_3N_4	50	Pt	350W Xe lamp (＞400 nm)	TEOA	18.7	-	[15]
WO_3/g-C_3N_4 /$Ni(OH)_x$	50	$Ni(OH)_x$	300W Xe lamp (＞400 nm)	TEOA	28.8	-	[16]
g-C_3N_4/Ag-SCN	50	Ag-SCN	3W LED (420 nm)	lactic acid	3.89	-	[17]
TiO_2/CNX-NSs	50	Pt	300W Xe lamp (≥400 nm)	TEOA	138.4	7.1±0.2% at 450 nm	This work

References:

[1] C. W. Yang, J. Q. Qin, Z. Xue, M. Z. Ma, X. Y. Zhang and R. P. Liu, *Nano Energy*, 2017, **41**, 1-9.

[2] X. Shi, M. Fujitsuka, Z. Lou, P. Zhang and T. Majima, *J. Mater. Chem. A*, 2017, **5**, 9671-9681.

[3] J. Ma, X. Tan, F. Jiang and T. Yu, *Catal. Sci. Technol.*, 2017, **7**, 3275-3282.

[4] Y. Zou, J. W. Shi, D. Ma, Z. Fan, L. Lu and C. Niu, *Chem. Eng. J.*, 2017, **322**, 435-444.

[5] Q. Zhang, H. Wang, S. Chen, Y. Su and X. Quan, *RSC Adv.*, 2017, **7**, 13223-13227.

[6] Q. Tay, X. Wang, X. Zhao, J. Hong, Q. Zhang, R. Xu and Z. Chen, *J. Catal.*, 2016, **342**, 55-62.

[7] A. Qu, X. Xu, H. Xie, Y. Zhang, Y. Li and J. Wang, *Mater. Res. Bull.*, 2016, **80**, 167-176.

[8] X. Wei, C. Shao, X. Li, N. Lu, K. Wang, Z. Zhang and Y. Liu, *Nanoscale*, 2016, **8**, 11034-11043.

[9] K. He, J. Xie, Z. Q. Liu, N. Li, X. Chen, J. Hu and X. Li, *J. Mater. Chem. A*, 2018, **6**, 13110-13122.

[10] J. Wen, J. Xie, R. Shen, X. Li, X. Y. Luo, H. Zhang, A. Zhang and G. Bi, *Dalton Trans.*, 2017, **46**, 1794-1802.

[11] K. He, J. Xie, M. Li and X. Li, *Appl. Surf. Sci.*, 2018, **430**, 208-217.

[12] J. Wen, J. Xie, Z. Yang, R. Shen, H. Li, X. Y. Luo and X. Chen, *ACS Sustain. Chem. Eng.*, 2017, **5**, 2224-2236.

[13] J. Wen, J. Xie, H. Zang, A. Zhang, Y. Liu, X. Chen and X. Li, *ACS Appl. Mater. Interfaces*, 2017, **9**, 14031-14042.

[14] X. L. Luo, G. L. He, Y. P. Fang and Y. H. Xu, *J. Colloid Interface Sci.*, 2018, **518**, 184-191.

[15] J. Jiang, S. Cao, C. Hu and C. Chen, *Chin. J. Catal.*, 2017, **38**, 1981-1989.

[16] K. He, J. Xie, X. Luo, J. Wen, S. Ma, X. Li, Y. Fang and X. Zhang, *Chin. J. Catal.*, 2017, **38**, 240-252.

[17] F. Chen, H. Yang, W. Luo, P. Wang and H. Yu, *Chin. J. Catal.*, 2017, **38**, 1990-1998.